Ammonia and nitrite oxidation in the upper euphotic zone of the oligotrophic Red Sea

Eyal Rahav[1,2,3*], Scott D Wankel[4], and Adina Paytan[2]

[1] Israel Oceanographic and Limnological Research, Haifa, Israel.
[2] Institute of Marine Science, University of California, Santa Cruz, CA, USA.
[3] Department of Earth and Environmental Science, Ben-Gurion University of the Negev, Beer Sheva, Israel.
[4] Marine Chemistry and Geochemistry Department, Woods Hole Oceanographic Institution, Woods Hole, Massachusetts, USA.

*Corresponding author: eyrahav@ucsc.edu; eyal.rahav@ocean.org.il

Abstract

Nitrification is widely understood to be inhibited by light in the surface ocean, however, increasing evidence indicates its occurrence at low levels at many sites. The extent to which nitrification remains active in the euphotic zone could have important implications to new production calculations, yet it remains understudied. Here, we quantified ammonia and nitrite oxidation rates in the euphotic zone of the Gulf of Aqaba (Northern Red Sea) from late spring to late summer and examined environmental controls and implications for dark carbon fixation (chemoautotrophy) and new production. Both ammonia and nitrite oxidation were detectable throughout the euphotic zone (~0.1-0.8 nmol N L^{-1} d^{-1}). Overall, rates were low in the highest-irradiance surface waters and increased with depth. Integrated rates over the entire euphotic zone (24-56 μmol N m^{-2} d^{-1}) were among the lowest reported for oligotrophic regions globally. This reflects extremely low substrate concentrations and intense, though not complete, photo-inhibition. Ammonia and nitrite oxidation together supported <2% of dark carbon fixation rates, suggesting other processes, not accounted for, drive this chemoautotrophic activity. Depth-resolved correlations with environmental parameters highlight light, temperature, and substrate availability as key regulators of both processes. Our results show that nitrification in the Gulf of Aqaba operates at the lower bounds of global euphotic zone rates and is loosely coupled to carbon cycling. These findings underscore the need to better resolve nitrification dynamics in ultra-oligotrophic, rapidly warming, seas to refine estimates of new production and chemoautotrophic carbon assimilation under future ocean conditions.

Key words: Ammonia oxidation, Nitrite oxidation, Dark carbon fixation, Red Sea, Oligotrophic.

1 Introduction

Nitrification, the sequential oxidation of ammonia (NH_4^+) to nitrite (NO_2^-) followed by the oxidation of nitrite to nitrate (NO_3^-), is a microbially mediated process central to the regulation of nitrogen availability across nearly all aquatic environments, linking the most reduced and oxidized states of nitrogen (Ward, 2008). Although nitrification does not change the absolute inventory of bioavailable nitrogen (N) in the oceans, it alters the balance among nitrogen species that serve as substrates for different organisms, thereby affecting phytoplankton species abundance and growth (Fawcett et al., 2011). Ammonia oxidation is carried out by ammonia-oxidizing archaea and bacteria (Francis et al., 2005; Wuchter et al., 2006), while nitrite oxidation is performed by nitrite-oxidizing bacteria (Mincer et al., 2007; Pachiadaki et al., 2017). Ammonia-oxidizing bacteria that perform the entire process have also been identified in freshwater, terrestrial, and coastal habitats, but have not yet been found in the open ocean (Daims et al., 2015; Fei et al., 2018; van Kessel et al., 2015).

Nitrification has been investigated across a wide range of marine settings, including the Atlantic (Clark et al., 2008, 2022), the Pacific (Wan et al., 2021; Wankel et al., 2007), and the Polar (Mdutyana et al., 2020; Shiozaki et al., 2019) ocean basins, as well as numerous coastal and estuarine systems (Henriksen and Kemp, 1988; Herbert, 1999; Zhu et al., 2018). As a chemoautotrophic process, nitrification contributes to organic carbon production in the ocean interior (Middelburg, 2011; Pachiadaki et al., 2017), and may fuel bacterial carbon demand and support heterotrophic food-webs in the mesopelagic and bathypelagic water depths (Bayer et al., 2025). The activity of nitrifiers is known to be promoted or inhibited by many environmental factors (Ward, 2008), yet specific controls on its occurrence in the water column and broader ecological implications across different ocean settings remain poorly constrained (Tang et al., 2023). Additionally, because uptake of NH_4^+ and NO_3^- has long served to differentiate between 'regenerated' and 'new' production, respectively (Eppley and Peterson, 1979), *in situ* production of NO_3^- by nitrification in the photic zone skews global estimates of new production and carbon export in the oceans (Yool et al., 2007; Wankel et al., 2007).

Here, we report ammonia and nitrite oxidation rates in the upper euphotic zone (surface and down to ~100 m, representing 100% to ~0.5-1.8% of surface irradiance, respectively) of

the Gulf of Aqaba (GoA, Northen Red Sea) during late spring and throughout the summer season. Rates were compared with common environmental physiochemical and biological parameters to assess drivers of nitrification in this marine setting. Using these data, we provide estimates of the contribution of ammonia and nitrite oxidation to dark carbon fixation (DCF) and new production in thr oligotrophic, warm and well-lit GoA.

2 Material and methods

Seawater was collected every 20 m throughout the euphotic zone (0-100 m depth) at an offshore, routinely monitored, station in the GoA ("Station A", latitude 29.47 N, longitude 34.92 E). Ammonia and nitrite oxidation rates were assessed using stable ^{15}N isotope enrichment incubations. Five monthly sampling events were performed spanning late spring/early summer (May) to late summer (September) in 2023, covering the period in which the GoA is characterized by oligotrophic N-poor conditions (Fuller et al., 2005; Mackey et al., 2007). Ancillary water column measurements included temperature, salinity, photosynthetic active radiation (PAR) (Seabird 19 Plus), inorganic nitrogen species concentrations (NO_2^-, NO_3^-, NH_4^+), chlorophyll-*a*, and rates of photosynthesis and DCF.

2.1 Inorganic nitrogen species

Duplicate water samples for nitrite (NO_2^-) and nitrate (NO_3^-) were collected in 15 ml acid-clean polyethylene tubes directly from Niskin bottles. Prior to filling, the tube was thoroughly rinsed three times with sample water. After collection, samples were stored at 4 °C in the dark and analyzed the following day. Nitrite (NO_2^-) and nitrate (NO_3^-) concentrations were determined colorimetrically following standard procedures (Grasshoff et al., 1999). Nitrite was measured directly using the Griess reaction, in which nitrite forms an azo dye after reaction with sulfanilamide and N-(1-naphthyl)ethylenediamine and is quantified spectrophotometrically (λ=520 nm). Nitrate was reduced to nitrite using a copper-coated cadmium reduction column and subsequently NO_2^-+NO_3^- was analyzed by the same azo-dye method. Nitrate concentrations were then calculated by difference. Analyses were performed using a Flow Injection Autoanalyzer system (FIA, Lachat Instruments Model QuikChem 8000). The analysis was automated, and peak areas were calibrated using standards prepared in nutrient-deplete 0.2-µm filtered surface seawater from the GoA over a range of 0-100 nmol L^{-1}. The detection limits were 10 nmol L^{-1} and 20 nmol L^{-1} for nitrite and nitrate, respectively, with typical analytical precision of ~20 nmol L^{-1}, consistent with previous measurements in the GoA (e.g., Mackey et al., 2011).

Samples for ammonia (NH_4^+) concentration were collected directly from Niskin bottles into acid-washed plastic vials after rinsing 3 times with sample water. The collected samples were stored in 4 °C in the dark and analyzed within an hour after collection. Ammonia concentrations were determined using the orthophthaldialdehyde (OPA) method (Holmes et al., 1999), where samples were first incubated with a working reagent of OPA for 3 h and then measured fluorometrically (Turner Designs, Ex: 360 nm, Em. 420 nm). The detection limit of the OPA analysis was ~4 nmol L^{-1} (Meeder et al., 2012).

Procedural blanks were routinely measured and subtracted from sample signals to account for background contamination. Note that calibration and quality control procedures were carried out during nutrient measurements. The analytical precision and detection limits were within the expected range for oligotrophic seawater measurements.

2.2 Ammonia and nitrite oxidation rates

Ammonia and nitrite oxidation rates were determined using stable isotope tracer incubations (Beman et al., 2011; Bristow et al., 2015; Ward, 1987). Seawater was collected into triplicate 1-L acid-cleaned transparent Nalgene bottles without headspace. The bottles were incubated on land for 24 h in aquarium tanks continuously supplied with running surface seawater, using neutral density screening nets simulating the light conditions of the collection depth (no change in spectra). For ammonia oxidation, samples were amended with ^{15}N-labeled ammonium chloride ($^{15}NH_4Cl$, >98 atom %; Cambridge Isotope Laboratories) at a concentration of ~20 nmol L^{-1} which is sufficient to yield a quantifiable signal while potentially introducing some degree of tracer perturbation (discussed below). For nitrite oxidation, samples were amended with ~5 nmol L^{-1} of ^{15}N-labeled sodium nitrite ($^{15}NO_2^-$, >98 atom %), thus minimally perturbing the *in situ* nitrite pool. At the end of the incubation, subsamples were filtered onto a Supor 0.22 μm (47 mm) filter using gentle filtration, and the filtrate (<0.22 μm) was kept frozen in the dark at -20 °C until analysis. For ammonia oxidation, the presence of $^{15}NO_2^-$ in the total dissolved nitrite pool was quantified by isotope ratio mass spectrometry (IRMS).

For nitrite oxidation, we quantified the $^{15}NO_3^-$ in the dissolved nitrate pool after conversion to nitrous oxide via the denitrifier method (Sigman et al., 2001) and subsequent IRMS analysis. Note that in order to ensure sufficient nitrogen mass for isotopic analysis under low ambient nutrient concentrations, relatively large incubation volumes (1 L) were used, and a substantial fraction of the filtrate was processed for isotope measurements. The azide and denitrifier methods employed here are well established for the analysis of low-concentration

nitrite and nitrate pools and allow reliable detection of ^{15}N enrichment in oligotrophic systems (Buchwald et al., 2018). Recent methodological modifications involving anion-exchange resin enrichment coupled with azide reduction for low-concentration nitrite isotope analysis were suggested to enhanced analytical sensitivity (Jiang et al., 2026); however, the established approaches used here are widely applied in oligotrophic systems and were sufficient for robust detection of ^{15}N enrichment in the present study.

Killed controls poisoned with $HgCl_2$ from each collection depth were incubated in parallel to the experimental bottles to account for any abiotic transformations and subtracted from the 'live' bottles. Rates in the 'mercury-killed' controls were typically negligible relative to the 'live' bottles (usually <0.05 nmol N L^{-1} d^{-1}). The resulting detection limit, which was defined as the mean killed-control rate plus three standard deviations, corresponded to 0.1 nmol N L^{-1} d^{-1}. Rates below this threshold were considered indistinguishable from background signal and were interpreted as 'below detection'.

Rates of ammonia and nitrite oxidation were calculated following previous studies (Beman et al., 2011; Bristow et al., 2015; Ward, 1987) as shown in Equations 1-3:

$$(1)\ \text{Ammonia oxidation} = \frac{\Delta\ (\text{atm\% 15N NO2})\ \text{x}\ [\text{NO2}]\text{final}}{\text{t x F (NH4)}}$$

$$(2)\ \text{Nitrite oxidation} = \frac{\Delta\ (\text{atm\% 15N NO3})\ \text{x}\ [\text{NO3}]\text{final}}{\text{t x F (NO2)}}$$

$$(3)\ \text{F substrate} = \frac{[15N\ substrate]added}{[\text{Substrate ambient}]+[\text{Substrate added}]}$$

Where, Δ(atm% ^{15}N NO_2^-) or Δ(atm% ^{15}N NO_3^-) = atom% excess ^{15}N in the nitrite or nitrate pool relative to natural abundance; $[NO_2^-]_{final}$ or $[NO_3^-]_{final}$ = final concentration of the nitrite or nitrate pool (nmol L^{-1}); t = time (d); F_{NH4} or F_{NO2} = fractional ^{15}N enrichment of the ammonia or nitrite substrate pool.

Note that for the ammonia oxidation rates we added tracer additions which correspond to 30-50% of the ambient NH_4^+ concentrations. While we aimed to minimize substrate perturbation, such additions are inherently challenging in ultra-oligotrophic systems, where even low absolute tracer concentrations can represent a substantial fraction of the ambient pool (Zheng et al., 2020). Consequently, the reported rates should be considered as potential rates

under moderately enriched conditions rather than strictly *in situ* rates (Dodds and Jones, 1987). Additionally, incubations were conducted over 24 h, which may allow for processes such as ammonia regeneration, microbial turnover, and grazing to influence substrate availability and isotopic dilution. Although $HgCl_2$-poisoned controls and parallel measurements were used to account for abiotic and background signals, these incubations cannot fully resolve short-term dynamics or transient coupling between regeneration and oxidation processes. These methodological constraints are inherent to low-rate measurements in oligotrophic systems (Ward, 1985) and should be considered when interpreting the results. Another potential cavate arising from the 24 h incubation is the potential production of unlabelled nitrite via phytoplankton nitrate reduction (e.g., Travis et al., 2024) thereby diluting the $^{15}NO_2^-$ pool leading to an underestimation of both ammonia and nitrite oxidation rates. In the present study, however, primary production and ambient nitrite concentrations were low, suggesting that this effect was likely limited in magnitude.

2.3 Photosynthesis and Dark Carbon Fixation (DCF)

Photosynthesis and chemoautotrophic DCF rates were measured using $NaH^{14}CO_3$ incorporation method (Steemann-Nielsen, 1952) with minor modifications (Reich et al., 2024, 2026). Triplicate seawater samples were collected from Niskin bottles in 50 ml acid-washed falcon tubes and spiked with a diluted 'working solution' of $NaH^{14}CO_3$ (Perkin Elmer, specific activity 56 mCi $mmol^{-1}$) at a final radioisotope dilution of $1{:}10^4$ *v:v.* Tubes were incubated in the same tanks and under the same conditions used for the ammonia and nitrite oxidation measurements with one exception – the DCF bottles were first covered with aluminum foil to prevent light penetration. The tubes were incubated for 24 h before being filtered onto GF/F filters (0.7 µm nominal pore size, 25 mm diameter) using low vacuum pressure (<50 mmHg). The filters were placed in glass scintillation vials and 50 µl of 37% hydrochloric acid was added to remove the non-fixed ^{14}C-bicarbonate overnight. Scintillation cocktail (5 ml, ULTIMA-GOLD) was then added to each vial and samples were counted using a TRI-CARB 4810 TR (Packard) liquid scintillation counter. Additional T_0 blanks were prepared by spiking bottles with $NaH^{14}CO_3$ and filtering immediately (without incubation). Blanks consistently yielded negligible activity. Added activity was measured by withdrawing 50 µl from random spiked bottles (immediately after dosing and before incubation) and adding it onto a new GF/F filter with 50 µl of ethanolamine (pH≈12) followed by scintillation cocktail and counting immediately.

196 Photosynthesis was calculated as the difference between the disintegration per minute
197 (DPM) measured in the samples incubated under ambient irradiance and the dark bottles. DCF
198 and photosynthesis rates were calculated based on the Bermuda Atlantic Time-series Study
199 (BATS) protocol using the following Equation 4:

200 (4) $Production = \frac{(DPM-blank)}{V} \times DIC \times \frac{AA\ vol}{TDPM} \times f \times \frac{1}{t}$

201 Where, DPM equals the disintegrations per minute, V = the filtered volume (50 ml), DIC is the
202 dissolved inorganic carbon in seawater (~25 mg C L^{-1}, similar to other oceanic sites, (Knap and
203 Michaels, 1993), AA vol = Added activity volume (50 µl), TDPM = Total ^{14}C disintegration
204 per minute, t = incubation time (24h), and f = factor correcting isotope fractionation during
205 uptake of ^{14}C (1.05).
206
207 **2.4 Chlorophyll.*a* analysis**
208 Seawater samples (250 ml) were filtered onto Whatman GF/F filters at low pressure
209 (<150 mbar), placed in glass vials and frozen in the dark at -20 °C. Chlorophyll.*a* was extracted
210 with 5 ml of cold acetone (90%) overnight and determined by the non-acidification method
211 (Welschmeyer, 1994) using a Turner Designs (Trilogy) fluorometer.
212
213 **2.5 Statistical analysis**
214 Pairwise relationships between environmental variables and process rates were
215 evaluated using Pearson correlation coefficients calculated across all individual observations,
216 including all sampled depths (0-100 m) and stations. No prior averaging by depth or profile
217 was applied. Because many variables co-vary with depth and season, these correlations should
218 be interpreted as measures of co-variation rather than independent or causal relationships. Full
219 Pearson correlation statistics (r, r^2, p-values) are provided in Supplementary Tables S1 and S2.
220 Statistical analyses were performed using Python.
221
222 **3 Results and discussion**
223 **3.1 Physiochemical and biological characteristics of the GoA during summertime**
224 Sampling spanned from late spring (May) to the end of summer (September) within the
225 euphotic zone (0-100 m) of the GoA. Surface temperatures ranged from ~25 °C in May to ~28
226 °C at the end of summer (September) and declined to ~23.5 °C at 100 m during all sampling
227 events (Figure 1A). Photosynthetic active radiation (PAR) levels ranged from ~1200-1950

μmol quanta m^{-2} s^{-1} at the surface and decreased exponentially to ~10-20 μmol quanta m^{-2} s^{-1} at 100 m (Figure 1B), corresponding to 0.5-1.8% of the surface irradiation levels. The corresponding diffuse attenuation coefficient (Kd) was ~0.03-0.04 m^{-1}, in agreement with previous observations from the GoA (Dishon et al., 2012; Stambler, 2006) as well as in other oligotrophic regimes (Stambler, 2012). Concentrations of NH_4^+ ranged from undetectable to 65 nmol L^{-1} (Figure 1C). The corresponding integrated NH_4^+ inventory (0-100 m) was lowest in May (1.68 μmol m^{-2}) and highest in July (~4.57 μmol m^{-2}) (Table 1). NO_2^- levels were generally low throughout the upper 100 m (from below detection to <20 nmol L^{-1}), except in September when nitrite increased with depth reaching ~45 nmol L^{-1} below 40 m (Figure 1D). Vertical NO_2^- profiles suggest active ammonia oxidation below the strongly lit surface waters, especially during September, although we cannot rule out expulsion of NO_2^- by phytoplankton under light limitation (Berube et al., 2023; Collos, 1998). The vertically integrated NO_2^- inventories ranged from 0.79-3.39 μmol m^{-2} (Table 1). Surface NO_3^- was also low (<20 nmol L^{-1}) and generally increased with depth, suggesting organic matter regeneration and nitrification during summertime (Figure 1E), and/or that less NO_3^- is assimilated by phytoplankton at deeper depths. The integrated NO_3^- inventory ranged from 2.65 μmol m^{-2} in May and September up to 10.36 μmol m^{-2} in June (Table 1). Collectively, the summertime inorganic N species concentrations in the upper 100 m were low, in agreement with previous reports from the oligotrophic GoA (Mackey et al., 2011; Meeder et al., 2012; Rahav et al., 2015).

Chlorophyll.*a* concentrations were low in the surface water (<0.15 μg L^{-1}) and gradually increased with depth reaching maximal values in May and June (~0.60 μg L^{-1}) (Figure 2A). The corresponding integrated chlorophyll.*a* was 26-28 mg m^{-2} except in August where it was 16 mg m^{-2} (Table 1). As expected, photosynthesis rates were highest in the surface water and decreased with depth (Figure 2B), coinciding with the decreasing PAR levels (Figure 1B). Photosynthesis rates decreased from ~10 μg C L^{-1} d^{-1} at the surface to below detection at 100 m, except in September when elevated rates were observed throughout the water column, ranging from ~10 to 25 μg C L^{-1} d^{-1} (Figure 2B). The resulting integrated photosynthesis rates ranged from 242 mg C m^{-2} d^{-1} in August to as high as 1263 mg C m^{-2} d^{-1} in September (Table 1). Despite the fluctuation in photosynthetic rates between months, these values are within the range previously reported from the GoA (Rahav et al., 2015; Reich et al., 2024; Suggett et al., 2009).

Chemoautotrophic DCF was lower than photosynthesis rates and exhibited no clear vertical trends (Figure 2C). The surface DCF ranged from ~0.2-0.6 μg C L^{-1} d^{-1} to ~0.1-0.9 μg

C L^{-1} d^{-1} at 100 m (Figure 2C). The resulting integrated DCF ranged from 17-37 mg C m^{-2} d^{-1}, in agreement with a recent study from the GoA (Reich et al., 2024), corresponding to ~3-10% of all the total autotrophic activity (photosynthesis and DCF combined). While multiple microbial metabolisms involve chemoautotrophic carbon fixation, DCF is primarily attributed to ammonia and nitrite oxidation, as these chemoautotrophic metabolisms are ubiquitous throughout the oxic water column (Middelburg, 2011; Tang et al., 2023). In general, ammonia oxidation likely provides energy that supports chemoautotrophic CO_2 assimilation throughout the euphotic zone. Though less energy efficient, nitrite oxidation also contributes to DCF and is considered especially relevant near the base of the euphotic zone where NO_2^- often accumulates and reaches a maximum in concentration (Tang et al., 2023).

Table 1: Summary of integrated values (0-100 m) measured in the GoA (N Red Sea) during summer 2023.

Variable	May 23	June 23	July 23	Aug. 23	Sept. 23
Mixed layer depth (m)*	45	31	21	15	28
NH_4^+ (µmol m^{-2})	1.68	4.54	4.57	3.36	2.99
NO_2^- (µmol m^{-2})	1.76	0.79	0.94	1.64	3.39
NO_3^- (µmol m^{-2})	2.76	10.36	6.60	6.13	2.65
Chlorophyll.*a* (mg m^{-2})	26	28	26	16	28
Photosynthesis (mg C m^{-2} d^{-1})	350	349	302	242	1263
DCF (mg C m^{-2} d^{-1})	32	17	35	27	37
NH_4^+ oxidation (µmol m^{-2} d^{-1})	28	48	39	45	56
NO_2^- oxidation (µmol m^{-2} d^{-1})	24	38	45	39	44
Contribution of NH_4^+ oxidation to DCF (%)**	0.32	1.02	0.40	0.60	0.54
Contribution of NO_2^- oxidation to DCF (%)***	0.05	0.13	0.08	0.09	0.07

* Calculated from a temperature threshold criterion (ΔT = 0.2 °C from surface values (de Boyer Montégut et al., 2004).

**Assuming 0.3 moles of C fixed per mole of NH_4^+ oxidized (Santoro et al., 2010).

***Assuming 0.05 moles of C per mole of NO_2^- oxidized (Beman et al., 2013).

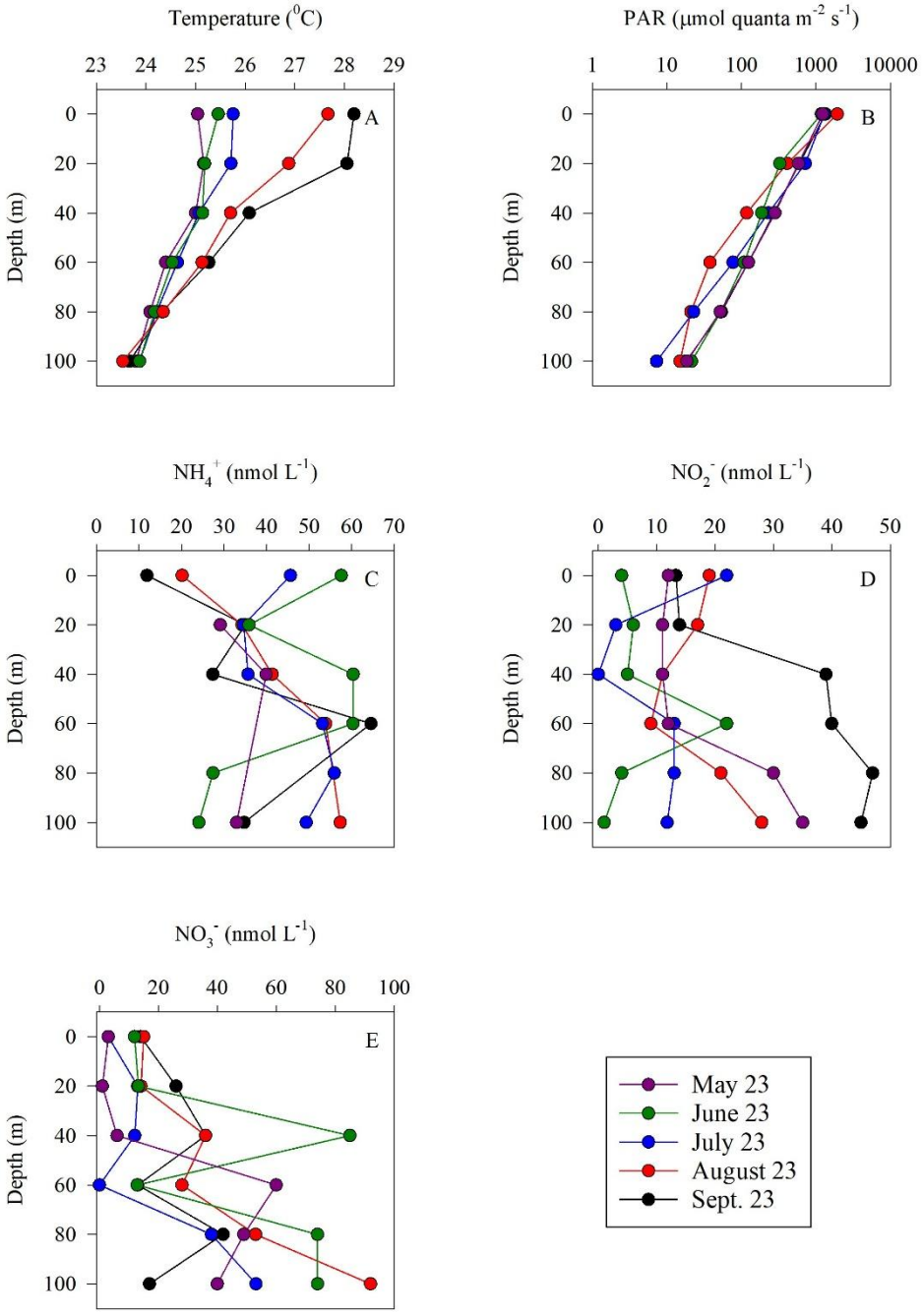

Figure 1: Vertical distribution of temperature (A), PAR (B), NH_4^+ (C), NO_2^- (D) and NO_3^- (E) in the upper euphotic zone in the GoA, N Red Sea between May and September 2023.

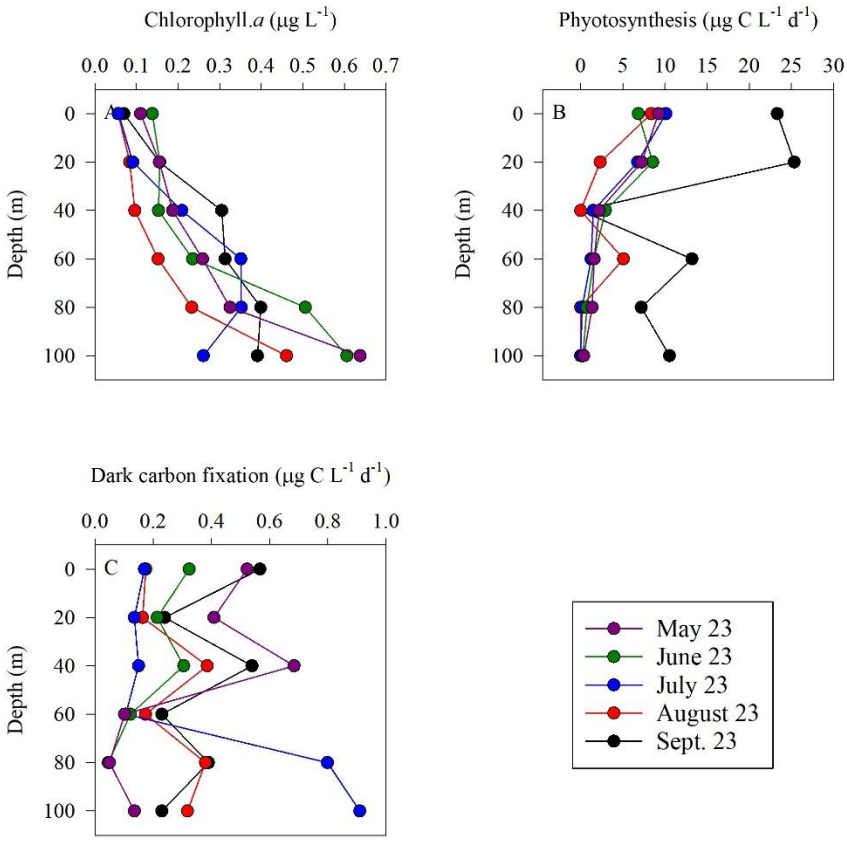

Figure 2: Vertical distribution of chlorophyll-a (A), photosynthesis (B), and dark carbon fixation (C) in the upper euphotic zone in the GoA, N Red Sea between May and September 2023.

3.2 Ammonia and nitrite oxidation rates

Ammonia and nitrite oxidation rates were generally low throughout the euphotic zone yet exhibited an increasing trend with depth (Figure 3), consistent with regulation by light inhibition. Overall, ammonia oxidation was homogeneous in the upper 40 m, ranging from ~0.10-0.55 nmol N L^{-1} d^{-1}. Below this depth rates increased towards the bottom of the euphotic zone (~100 m), ranging from ~0.26-0.83 nmol N L^{-1} d^{-1} (Figure 3A,B). Ammonia oxidation rates often reached a maximum near the base of the euphotic zone (below the 50-100 m layer) as seen in other studies (reviewed by Tang et al., 2023). In general, these low euphotic zone ammonia oxidation rates are consistent with light inhibition, given the high PAR of the GoA during summer (Figure 1B, Wan et al., 2021). Competition of nitrifiers with phytoplankton for NH_4^+ may also result in low ammonia oxidation rates, as has been reported in the surface sunlit North Pacific (Smith et al., 2014). However, the highest integrated ammonia oxidation rate (September, 56 µmol m^{-2} d^{-1}) was measured when chlorophyll.*a* levels and primary productivity were also relatively high and similar to springtime when the lowest ammonia

oxidation rates were measured (May, 28 μmol m^{-2} d^{-1}) (Table 1). Thus, competition between nitrifiers and phytoplankton for NH_4^+ does not appear to play a direct role in the regulation of oxidation rates in our study. That said, the lack of correlation between chlorophyll *a* and ammonia (R^2=0.003) does not preclude competition, but instead likely reflects rapid recycling and tight coupling between ammonium production and uptake. Ammonia oxidation rates have also been shown to be influenced by trace metal availability, specifically iron and copper (Martocello and Wankel, 2024; Shafiee et al., 2019, 2021). However, given the close proximity to major deserts, iron is not considered a limiting factor for microbes in the surface water of the GoA (Chen et al., 2008; Torfstein et al., 2017). The limiting factors for ammonia oxidizers in the GoA should be further studied by simulating different nutrients and temperature scenarios with or without amendments of an inhibitor of ammonia monooxygenase to better examine controls on environmental rates(Bayer et al., 2025).

During the study period, the mixed layer depth shoaled from ~45 m in May to ~15 m in August (Table 1), reflecting progressive seasonal stratification. The vertical pattern of ammonia oxidation (Figure 3) suggests that rates remained low throughout the strongly illuminated upper water column, while modest increases at 60–80 m likely reflected reduced light inhibition and/or more favorable conditions for nitrifier activity below the mixed layer. Thus, unlike systems where ammonia oxidation increases sharply below the deep chlorophyll maximum, nitrification in the GoA appears to follow a more gradual depth-related response during stratified conditions.

As with ammonia oxidation, rates of nitrite oxidation also increased with depth (Figure 3C,D). Nitrite oxidation ranged from 0.14 to 0.70 nmol L^{-1} d^{-1} (Figure 3C,D), with highest rates measured over 80-100 m. Integrated nitrite oxidation rates were lowest in spring/early summer (~24 μmol m^{-2} d^{-1}) and increased between June to September (38-45 μmol m^{-2} d^{-1}) (Table 1). Nitrite oxidation maxima (~100 m) were deeper than those of ammonia oxidation (~60 m). This vertical offset may reflect differences in substrate supply and the decoupling of ammonia and nitrite oxidation along the water column in addition to differential sensitivity to light (Wan et al., 2021). For example, ammonium supply may be more closely linked to shallower regeneration processes, whereas nitrite can accumulate and persist at greater depths (Travis et al., 2024).

Our results demonstrate that ammonia and nitrite oxidation occurred at comparable rates, which is consistent with the typically low concentrations of NO_2^- observed in the GoA during summertime (Figure 1D, Meeder et al., 2012), and consistent with the low net accumulation of NO_2^- resulting from limited decoupling between the two steps of nitrification.

Converting photosynthesis to nitrogen demand using Redfield stoichiometry (C:N ≈ 6.6) suggests that phytoplankton nitrogen requirements in surface waters may substantially exceed the measured nitrification rates. This implies that regenerated nitrogen, including ammonium, is rapidly consumed, potentially limiting its availability for ammonia-oxidizing microorganisms. However, this inference is based on carbon-derived estimates of phytoplankton demand rather than direct measurements of nitrogen uptake and should therefore be interpreted cautiously. Nevertheless, previous studies indicate that ammonia uptake can greatly exceed nitrification rates in oligotrophic surface waters (Mackey et al., 2011).

To assess substrate control, we examined the relationship between NH_4^+ concentration and ammonia oxidation rates across depths. This relationship was weak overall (Pearson, r≈0.30), whereas rates were more strongly associated with depth (r≈0.75), indicating a dominant role of depth-related gradients (Figure S1, Table S1). When examined by depth intervals (0-50 m vs. 50-100 m), the NH_4^+–oxidation relationship was weak in the upper 50 m (r≈0.23) and stronger >50 m (r≈0.41) (Figure S1, Table S1). This suggests that rapid recycling and competitive uptake weaken NH_4^+– oxidation rate coupling in surface waters, whereas reduced light inhibition at depth allows a somewhat greater influence of NH_4^+. These results are consistent with previous studies showing that nitrification maxima are often decoupled from NH_4^+ peaks and instead reflect depth-dependent ecological structuring (Beman et al., 2012).

Note that a key consideration in interpreting the measured rates is the relative magnitude of the $^{15}NH_4^+$ tracer addition compared to ambient substrate concentrations. In the upper euphotic zone, where NH_4^+ concentrations were often near detection limits (Figure 1), the addition of ~20 nmol L^{-1} (tracer) represented a substantial enrichment of the available pool. Under such conditions, if ammonia oxidation were strongly substrate-limited, one might expect a measurable stimulation of rates. However, the observed rates remained consistently low across depths and sampling periods (Table 1; Figure 3), even under these 'enriched' conditions. This suggests that factors other than immediate substrate availability exert primary control over ammonia oxidation in the upper waters of the GoA. These may include low abundances of ammonia-oxidizing archaea (Aizawa et al., 2023; Smith et al., 2016), strong light inhibition in surface waters (Figure 1B), or physiological constraints associated with oligotrophic adaptation (Yin et al., 2024; Zhou et al., 2024). Rather than indicating the absence of substrate limitation *per se*, our results imply that ammonia oxidation operates under a combination of ecological and environmental constraints that limit its overall contribution to nitrogen cycling in this system. Moreover, the use of 24 h incubations introduce additional uncertainty, as internal

recycling of ammonium and microbial interactions may partially decouple measured rates from instantaneous *in situ* conditions. Therefore, the rates reported here are interpreted as conservative estimates of nitrification potential in the upper euphotic zone. Adding to that, in oligotrophic systems, rapid recycling of dissolved inorganic nitrogen can influence both substrate availability (Christie-Oleza et al., 2017) and isotopic enrichment during incubation experiments (Stukel, 2020). Thus, processes such as ammonium regeneration and microbial uptake may dilute the ^{15}N substrate pool or reduce accumulation of labelled products (Braun et al., 2018). However, we surmise that any such processes, if occurred here, would tend to reduce the apparent isotopic enrichment and thus bias rate estimates toward underestimation. Another possible limitation regards the uncertainty in low nutrient concentrations in the GoA (most notably within the upper mixed layer depth) that may propagate into rate calculations, as substrate concentrations are explicitly included in the rate equations (see equations 1-3). However, such uncertainty affects absolute rate estimates proportionally and does not alter the overall interpretation of low nitrification activity. Accordingly, the reported rates should be considered conservative estimates of nitrification activity over the incubation period.

3.3 Contribution of ammonia and nitrite oxidation to DCF

DCF is widely thought to be dominated by ammonia and nitrite oxidation, as these metabolic processes provide energy that, in turn, support chemoautotrophic CO_2 assimilation (Middelburg, 2011), although additional pathways such as urea oxidation by ammonia oxidizers may also contribute (Wan et al., 2024). While other chemoautotrophic metabolisms, such as sulfur oxidation, anammox or methanotrophy also represent important drivers of chemoautotrophy in some environments, these are unlikely to be relevant in the oxic, oligotrophic waters of the GoA. DCF and nitrification are rarely measured simultaneously, which prevents robust assessment of this relationship. Here, we explored DCF under the warm, high-light, nutrient-poor conditions found in the GoA (Figure 1) and investigated how it relates to corresponding rates of nitrification over the euphotic zone. We calculated the contribution of ammonia and nitrite oxidation to DCF assuming 0.3 moles of C fixed per mole of NH_4^+ (Santoro et al., 2010). Overall, the depth-integrated contribution of ammonia oxidation to DCF ranged between 0-2%, consistent, yet often lower than reports from other oceanographic settings. For example, ammonia oxidizers contributed only a small fraction to DCF in the eastern tropical Pacific, accounting for <20% of depth-integrated rates (Bayer et al., 2025). The depth-integrated contribution of nitrite oxidation to DCF was negligible, accounting for 0.05-0.13% (Table 1). Thus, ammonia and nitrite oxidation together could account for only ~1% of

the DCF, lower than recent estimates from the eastern tropical Pacific (Bayer et al., 2025), though similar to observations in culture experiments with ammonia oxidizers (Bayer et al., 2023). It is notable, however, that relevant conversion factors between moles C fixed per mole of N oxidized in the ocean should be better constrained (and may be site-specific) (Tang et al., 2023), which could alter the calculated contribution discussed here. Nevertheless, we show that ammonia and nitrite oxidation link N recycling with inorganic carbon assimilation in the euphotic zone in the GoA, and while their contribution to total primary production is relatively small, it may sustain part of the microbial metabolism in the nutrient-depleted surface waters of the GoA. Our results suggest that other microbial metabolism processes (e.g., anaplerosis) may also contribute to DCF in the GoA's euphotic zone and should be estimated separately in future studies.

DCF in the sunlit ocean should not be interpreted solely as nitrification-driven chemoautotrophy. Even under dark incubation conditions, inorganic carbon fixation may include contributions from phytoplankton-associated dark metabolism, heterotrophic inorganic carbon assimilation, and other microbial pathways (Baltar and Herndl, 2019; Reich et al., 2026). A recent 10-year analysis from the GoA (same study site) showed that DCF is a persistent but variable component of carbon cycling, contributing substantially to total autotrophic carbon fixation (Reich et al., 2024). Therefore, while our data suggests that ammonia and nitrite oxidation contribute only a minor fraction of total DCF, the remaining DCF signal likely reflects multiple unresolved microbial processes (Reich et al., 2025).

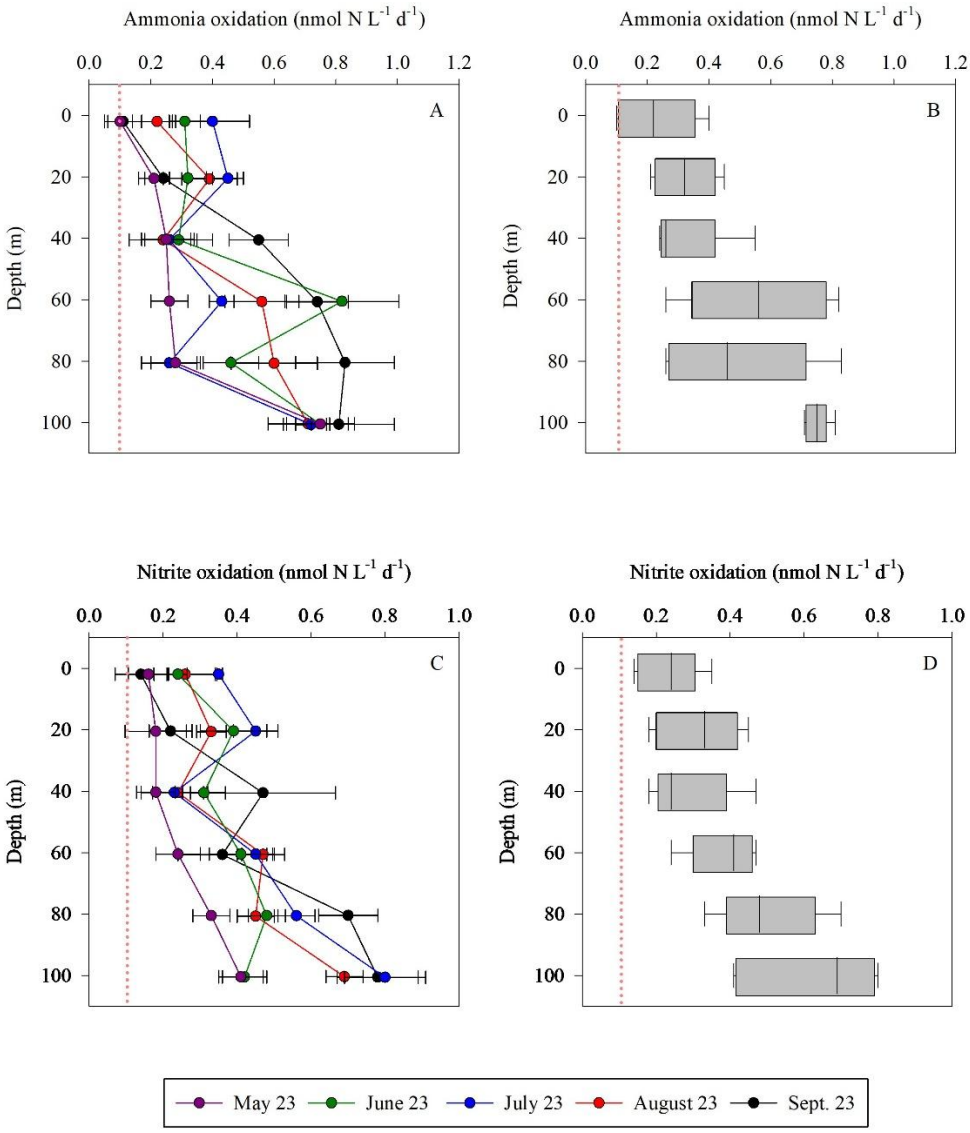

Figure 3: Vertical distribution of ammonia oxidation (A,B) and nitrite oxidation (C,D) in the upper euphotic zone in the GoA, N Red Sea between May and September 2023. The Box Wisker plots sum the data distribution per depth (n=5). The pink dashed line signifies the detection limit.

3.4 Environmental divers affecting ammonia and nitrite oxidation

Nitrification is known to be affected by PAR, oxygen levels, temperature, nitrogen substrate availability, pH, as well as by other environmental factors (Ward, 2008). Our results are consistent overall with previous observations at other sites as both ammonia and nitrite oxidation rates linearly correlate with most of these environmental variables, either positively or negatively (Figure 4; Figure S1; Tables S1 and S2). Most notably, ammonia and nitrite oxidation rates correlated with increasing depth and decreasing PAR level, consistent with previous reports showing that light inhibit nitrifier growth and nitrification rates (Merbt et al.,

2012; Olsen, 1989; Xu et al., 2019). Temperature correlated negatively with ammonia and nitrite oxidation rates (Figure 4, $r=0.61$, $p<0.01$), likely reflects substrate limitation rather than a direct temperature effect. Previous studies showed that increasing temperature generally stimulates nitrification by simultaneously altering substrate availability and enzyme kinetics (Emerson et al., 1975). As temperature increases, the pKa of the NH_4^+-NH_3 system decreases, shifting the equilibrium toward NH_3, the putative substrate of ammonia monooxygenase (Emerson et al., 1975). In parallel, warming enhances enzymatic activity, accelerating the catalytic steps of both ammonia and nitrite oxidation (Zheng et al., 2017, 2020). We surmise that in the stratified GoA, warming strengthened stratification, enhanced photo-inhibition, and thereby increased biological competition for ammonium, thus reducing substrate supply to nitrifiers despite favorable enzyme kinetics, leading to the observed negative correlation between temperature and nitrification. In agreement with this line of thought, substrate availability was positively correlated with ammonia oxidation (NH_4^+, NO_2^-) and nitrite oxidation (NO_2^-, NO_3^-), highlighting the substrate-dependent nature of nitrification. Alternatively, these relationships may reflect co-variation with depth and associated environmental gradients, rather than direct substrate control alone (discussed below). Ammonia oxidation requires NH_4^+ or NH_3 as the electron donor, while nitrite oxidation depends on NO_2^- availability. Elevated ambient concentrations of these substrates make them more available to nitrifying enzymes, resulting in higher reaction rates until enzymatic saturation or co-limitation with other nutrients are reached (e.g., vitamins and other co-factors, PO_4^+). In oligotrophic systems such as the GoA, where ambient NH_4^+ and NO_2^- concentrations are exceptionally low, even small pulses of reduced or intermediate nitrogen (e.g., from organic matter remineralization, mixing, or atmospheric deposition) may trigger an increase in nitrification rates.

Nitrification is generally expected to show a negative relationship with chlorophyll.*a* in surface waters, where phytoplankton may compete with nitrifiers for reduced nitrogen species. Consequently, most studies report suppressed ammonia and nitrite oxidation rates near the surface and enhanced rates below the chlorophyll maximum once light levels decrease and substrate regeneration through organic matter remineralization becomes more important (Beman et al., 2013; Yool et al., 2007). Here, however, we observed a positive correlation between chlorophyll.*a* and ammonia or nitrite oxidation (as well as with photosynthesis, although not significantly). This pattern likely reflects conditions near the deep chlorophyll maximum (~80-100 m), where chlorophyll *a* is elevated due to photo-acclimation under low light conditions rather than strictly higher biomass (Cornec et al., 2021; Fennel and Boss, 2003;

Scofield et al., 2020). In these depths, reduced irradiance and enhanced organic matter turnover may promote ammonium regeneration, providing substrate that supports nitrification. These findings suggest that the expected negative coupling at the surface is offset by strong regeneration and oxidation processes near the deep chlorophyll maxima, resulting in an overall positive relationship when integrated across the euphotic zone.

We expected that ammonia and nitrite oxidation would show a significant correlation with DCF (see discussion above). Nevertheless, although both ammonia and nitrite oxidation were positively coupled with DCF ($r=0.49$ and 0.17, respectively), the correlations were not statistically significant ($p>0.05$) and is in line with the overall low contribution of these processes to DCF (discussion above and see Table 1). This suggests that additional pathways such as anaplerotic processes may contribute to DCF (Dijkhuizen and Harder, 1984; Erb, 2011), as well as other chemoautotrophic metabolisms beyond nitrification such as urea oxidation, sulfur oxidation and iron oxidation (Arandia-Gorostidi et al., 2024; Dang and Chen, 2017), while the contribution of ammonia and nitrite oxidation to total DCF is low (Table 1).

We note that correlation analysis should be interpreted with caution. Many parameters considered here co-vary with depth (e.g., PAR, chlorophyll.*a*) and seasonal stratification (mixed layer depth), which can produce strong apparent relationships without implying direct mechanistic coupling. Furthermore, as the dataset is restricted to the upper 100 m, it does not capture the full vertical structure of nitrification, including deeper maxima often observed below the deep chlorophyll maximum. Accordingly, these correlations primarily reflect processes operating within the upper euphotic zone and should not be extrapolated beyond this depth range. Lastly, while variations in ammonia oxidation rates broadly co-occurred with changes in primary production and chlorophyll *a*, these relationships should be interpreted with caution. In this study, phytoplankton activity was assessed using carbon-based proxies, and no direct measurements of nitrogen uptake or community composition were conducted. Therefore, any inferred coupling between phytoplankton dynamics and nitrification remains indirect. The observed patterns are consistent with the expectation that phytoplankton influence the availability and cycling of regenerated nitrogen, but do not allow us to disentangle the relative roles of substrate competition, regeneration, or microbial community structure. Future studies that combine measurements of phytoplankton nitrogen demand, ammonium regeneration, and nitrifier abundance and activity will be required to directly resolve these interactions in oligotrophic systems.

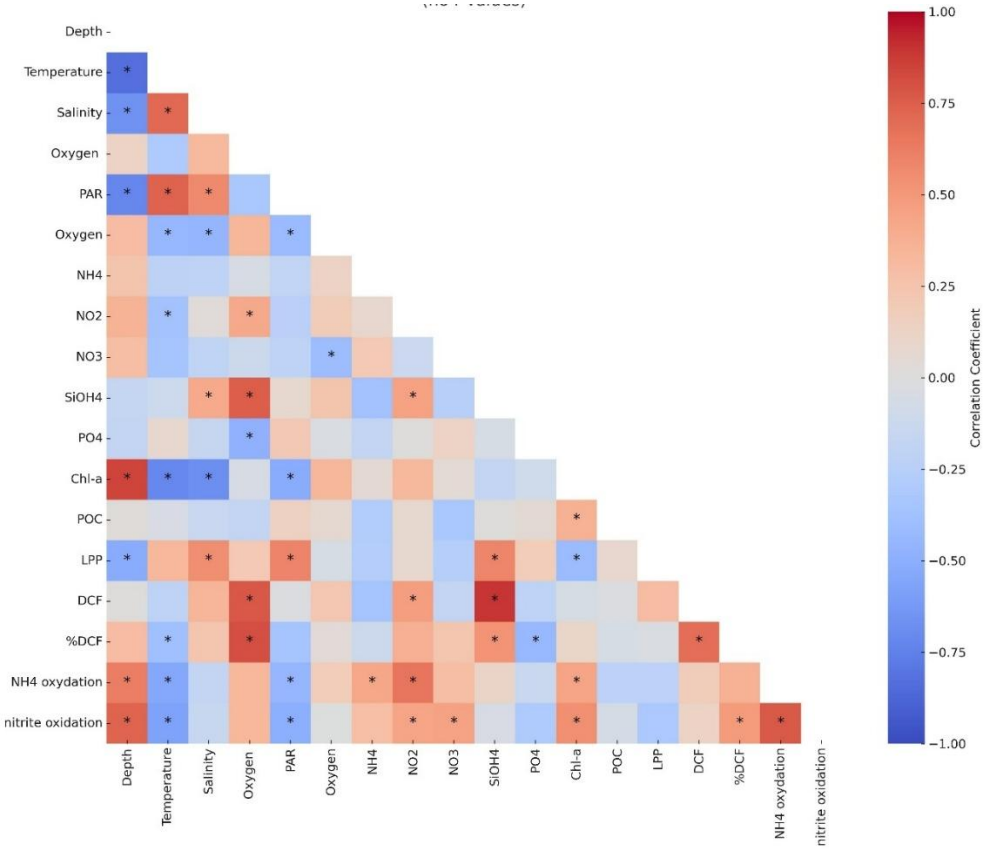

Figure 4: A heatmap showing Pearson correlation coefficients among measured environmental parameters and biogeochemical rates. Color shading indicates the strength and direction of the correlation. Asterisks denote statistically significant correlations ($p < 0.05$). Full descriptive statistics for the correlations are provided in the Supplementary Tables S1 and S2.

4 Conclusions

Globally, ammonia and nitrite oxidation rates in the euphotic zone span several orders of magnitude across offshore oceanic environments (Tang et al., 2023, Figure 5). The rates we measured in the GoA during summer fall below the global median (i.e., the red vs. black lines in Figure 5). The reason for the low rates in GoA is attributed to the low substrate availability during summertime (Figure 1C-E) but likely reflect a combination of environmental and ecological constraints rather than a single controlling factor. For example, the combination of high light intensity (Figure 1B) and penetration (i.e., $Kd \approx 0.04\ m^{-1}$) and enhanced stratification (Figure 1A) can further suppress nitrifier activity, either through photoinhibition of ammonia monooxygenase and/or by pushing microbial communities closer to their thermal tolerance limits. Moreover, the absence of measurements of nitrifier abundance preclude us from distinguishing whether low bulk rates reflect low population size or potentially high per-cell activity.

Additionally, while our results suggest a potential linkage between phytoplankton activity and nitrogen cycling, this inference is based on carbon-derived proxies (primary production and chlorophyll.*a*) rather than direct measurements of species-specific nitrogen uptake or microbial community composition using genetic markers. Resolving this coupling will require future studies that simultaneously quantify phytoplankton nitrogen demand, ammonium regeneration, and nitrifier abundance and activity.

Future studies should focus on resolving the temporal and spatial variability of nitrification rates and nitrifier communities in the context of ongoing climate change. This is especially true for the GoA that experience rapid warming and ocean acidification. Long-term time series and diel-scale observations are needed to capture seasonal, interannual, and daily dynamics, particularly in relation to stratification, warming, and nutrient supply. Advanced molecular approaches such as metagenomics, metatranscriptomics, and single-cell tools should be applied to link community composition and functional potential with *in-situ* rate measurements. Parallel measurements of trace metals will be essential to assess their role as cofactors or inhibitors of key enzymes in ammonia and nitrite oxidation. Furthermore, the contribution of nitrification to DCF appears to be limited, suggesting that additional microbial pathways contribute to inorganic carbon fixation in this system. Constraining these contributions will require future studies that integrate rate measurements with microbial community and metabolic analyses to better resolve the sources of DCF in oligotrophic waters. Ultimately, combining high-resolution field observations with targeted manipulations and modelling will improve our ability to predict how nitrification responds to environmental change and contributes to current and future ocean nitrogen cycling.

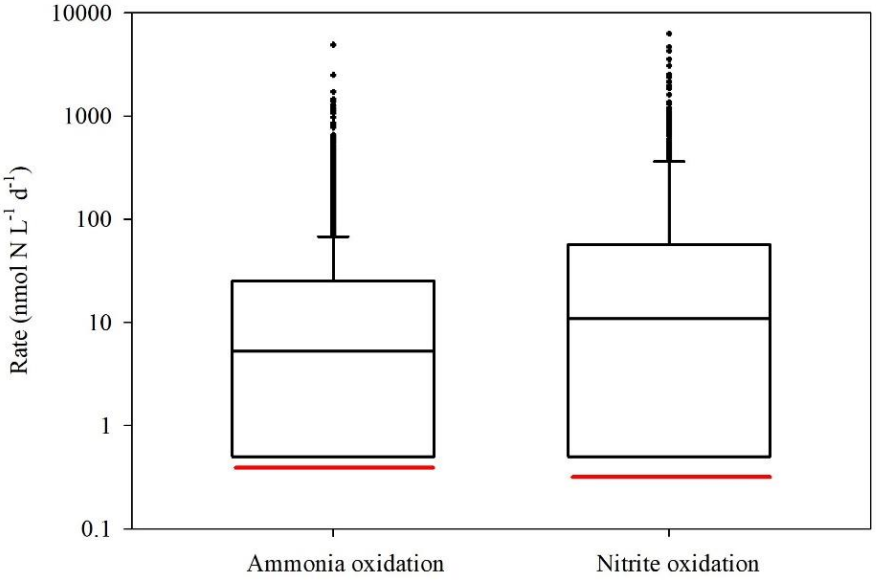

Figure 5: A literature compilation of reported euphotic zone's ammonia oxidation and nitrite oxidation recently reviewed Tang et al., (2023) and this study. The black line inside the boxes shows the median value of all studies considered, while the red line indicates the median values measured in the GoA during this study. Data include only offshore euphotic-zone measurements as defined in the original studies. We note that the depth and definition of the euphotic zone vary among regions, which may contribute to variability in reported rates.

Data availability. All the data is presented in the graphs/table/text and will be made available in excel format upon request.

Author contributions. Conceptualized and conducted the field measurements; ER. Data curation, formal analysis, and visualization; ER, SDW and AP. The paper was prepared by ER, SDW and AP.

Competing interests. The contact author has declared that none of the authors has any competing interests.

Acknowledgments. The authors thank the personnel in the Inter University Institute for Marine Sciences in Eilat (IUI). This paper was supported by a grant from the Middle East Regional Cooperation (MERC) (M39-011) to ER and AP. We also thank the two anonymous reviewers for their constructive comments, which helped to significantly improve and refine the manuscript.

References

Aizawa, A., Watanabe, Y., Hashioka, K., Kadoya, A., Suzuki, S., Yoshimura, T., and Kudo, I.: Contribution of ammonium oxidizing archaea and bacteria to intensive nitrification during summer in Mutsu Bay, Japan, Reg. Stud. Mar. Sci., 63, 102984, https://doi.org/https://doi.org/10.1016/j.rsma.2023.102984, 2023.

Arandia-Gorostidi, N., Jaffe, A. L., Parada, A. E., Kapili, B. J., Casciotti, K. L., Salcedo, R. S. R., Baumas, C. M. J., and Dekas, A. E.: Urea assimilation and oxidation support activity of phylogenetically diverse microbial communities of the dark ocean, ISME J., 18, https://doi.org/10.1093/ismejo/wrae230, 2024.

Baltar, F. and Herndl, G.: Is dark carbon fixation relevant for oceanic primary production estimates?, Biogeosciences Discuss., 1–12, https://doi.org/10.5194/bg-2019-223, 2019.

Bayer, B., McBeain, K., Carlson, C. A., and Santoro, A. E.: Carbon content, carbon fixation yield and dissolved organic carbon release from diverse marine nitrifiers, Limnol. Oceanogr., 68, 84–96, https://doi.org/https://doi.org/10.1002/lno.12252, 2023.

Bayer, B., Kitzinger, K., Paul, N. L., Albers, J. B., Saito, M. A., Wagner, M., Carlson, C. A., and Santoro, A. E.: Minor contribution of ammonia oxidizers to inorganic carbon fixation in the ocean, Nat. Geosci., 18, 1144–1151, https://doi.org/10.1038/s41561-025-01798-x, 2025.

Beman, J. M., Chow, C.-E., King, A. L., Feng, Y., Fuhrman, J. A., Andersson, A., Bates, N. R., Popp, B. N., and Hutchins, D. A.: Global declines in oceanic nitrification rates as a consequence of ocean acidification, Proc. Natl. Acad. Sci., 108, 208–213, https://doi.org/10.1073/pnas.1011053108, 2011.

Beman, J. M., Leilei Shih, J., and Popp, B. N.: Nitrite oxidation in the upper water column and oxygen minimum zone of the eastern tropical North Pacific Ocean, ISME J., 7, 2192–2205, https://doi.org/10.1038/ismej.2013.96, 2013.

Berube, P. M., J., O. T., Anna, R., Trent, L., and W., C. S.: Production and cross-feeding of nitrite within Prochlorococcus populations, MBio, 14, e01236-23, https://doi.org/10.1128/mbio.01236-23, 2023.

de Boyer Montégut, C., Madec, G., Fischer, A. S., Lazar, A., and Iudicone, D.: Mixed layer depth over the global ocean: An examination of profile data and a profile-based climatology, J. Geophys. Res. Ocean., 109, C12003, https://doi.org/https://doi.org/10.1029/2004JC002378, 2004.

Braun, J., Mooshammer, M., Wanek, W., Prommer, J., Walker, T. W. N., Rütting, T., and Richter, A.: Full 15N tracer accounting to revisit major assumptions of 15N isotope pool dilution approaches for gross nitrogen mineralization, Soil Biol. Biochem., 117, 16–26, https://doi.org/https://doi.org/10.1016/j.soilbio.2017.11.005, 2018.

Bristow, L. A., Sarode, N., Cartee, J., Caro-Quintero, A., Thamdrup, B., and Stewart, F. J.: Biogeochemical and metagenomic analysis of nitrite accumulation in the Gulf of Mexico hypoxic zone, Limnol. Oceanogr., 60, 1733–1750, https://doi.org/https://doi.org/10.1002/lno.10130, 2015.

Buchwald, C., Homola, K., Spivack, A. J., Estes, E. R., Murray, R. W., and Wankel, S. D.: Isotopic constraints on nitrogen transformation rates in the deep sedimentary marine biosphere, Global Biogeochem. Cycles, 32, 1688–1702, https://doi.org/https://doi.org/10.1029/2018GB005948, 2018.

Chen, Y., Paytan, A., Chase, Z., Measures, C., Beck, A. J., Sañudo-Wilhelmy, S. A., and Post, A. F.: Sources and fluxes of atmospheric trace elements to the Gulf of Aqaba, Red Sea, J. Geophys. Res. Atmos., 113, 1–13, https://doi.org/10.1029/2007JD009110, 2008.

Christie-Oleza, J. A., Sousoni, D., Lloyd, M., Armengaud, J., and Scanlan, D. J.: Nutrient recycling facilitates long-term stability of marine microbial phototroph-heterotroph interactions, Nat. Microbiol., 2, 17100, https://doi.org/10.1038/nmicrobiol.2017.100, 2017.

Clark, D. R., Rees, A. P., and Joint, I.: Ammonium regeneration and nitrification rates in the oligotrophic Atlantic Ocean: Implications for new production estimates, Limnol. Oceanogr., 53, 52–62, https://doi.org/https://doi.org/10.4319/lo.2008.53.1.0052, 2008.

Clark, D. R., Rees, A. P., Ferrera, C. M., Al-moosawi, L., Somerfield, P. J., Harris, C., Quartly, G. D., Goult, S., Tarran, G., and Lessin, G.: Nitrite regeneration in the oligotrophic Atlantic Ocean, Biogeosciences, 19, 1355–1376, https://doi.org/https://doi.org/10.5194/bg-19-1355-2022, 2022.

Collos, Y.: Nitrate uptake, nitrite release and uptake, and new production estimates, Mar. Ecol. Prog. Ser., 171, 293–301, 1998.

Cornec, M., Claustre, H., Mignot, A., Guidi, L., Lacour, L., Poteau, A., D'Ortenzio, F., Gentili, B., and Schmechtig, C.: Deep chlorophyll maxima in the global ocean: occurrences, drivers and characteristics, Glob. Biochem. cycles, 35, e2020GB006759, https://doi.org/10.1029/2020GB006759, 2021.

Daims, H., Lebedeva, E. V, Pjevac, P., Han, P., Herbold, C., Albertsen, M., Jehmlich, N., Palatinszky, M., Vierheilig, J., Bulaev, A., Kirkegaard, R. H., von Bergen, M., Rattei, T., Bendinger, B., Nielsen, P. H., and Wagner, M.: Complete nitrification by Nitrospira bacteria, Nature, 528, 504–509, https://doi.org/10.1038/nature16461, 2015.

Dang, H. and Chen, C.-T. A.: Ecological energetic perspectives on responses of nitrogen-transforming chemolithoautotrophic microbiota to changes in the marine environment, Front. Microbiol., 8, 1246, https://doi.org/10.3389/fmicb.2017.01246, 2017.

Dijkhuizen, L. and Harder, W.: Current views on the regulation of autotrophic carbon dioxide fixation via the Calvin cycle in bacteria, Antonie Van Leeuwenhoek, 50, 473–487, 1984.

Dishon, G., Dubinsky, Z., Caras, T., Rahav, E., Bar-Zeev, E., Tzubery, Y., and Iluz, D.: Optical habitats of ultraphytoplankton groups in the Gulf of Eilat (Aqaba), Northern Red Sea, Int. J. Remote Sens., 33, 2683–2705, https://doi.org/10.1080/01431161.2011.619209, 2012.

Dodds, W. K. and Jones, R. D.: Potential rates of nitrification and denitrification in an oligotrophic freshwater sediment system, Microb. Ecol., 14, 91–100, 1987.

Emerson, K., Russo, R. C., Lund, R. E., and Thurston, R. V: Aqueous ammonia equilibrium calculations: effect of pH and temperature, J. Fish. Res. Board Canada, 32, 2379–2383, https://doi.org/10.1139/f75-274, 1975.

Eppley, R. W. and Peterson, B. J.: Particulate organic matter flux and planktonic new production in the deep ocean, Nature, 282, 677–680, https://doi.org/10.1038/282677a0, 1979.

Erb, T. J.: Carboxylases in natural and synthetic microbial pathways, https://doi.org/10.1128/AEM.05702-11, December 2011.

Fawcett, S. E., Lomas, M. W., Casey, J. R., Ward, B. B., and Sigman, D. M.: Assimilation of upwelled nitrate by small eukaryotes in the Sargasso Sea, Nat. Geosci., 4, 717–722,

https://doi.org/10.1038/ngeo1265, 2011.

Fei, X., Jian-Gong, W., Ting, Z., Bin, Z., Sung-Keun, R., and Zhe-Xue, Q.: Ubiquity and diversity of complete ammonia oxidizers (Comammox), Appl. Environ. Microbiol., 84, e01390-18, https://doi.org/10.1128/AEM.01390-18, 2018.

Fennel, K. and Boss, E.: Subsurface maxima of phytoplankton and chlorophyll: Steady-state solutions from a simple model, Limnol. Oceanogr., 48, 1521–1534, https://doi.org/https://doi.org/10.4319/lo.2003.48.4.1521, 2003.

Francis, C. A., Roberts, K. J., Beman, J. M., Santoro, A. E., and Oakley, B. B.: Ubiquity and diversity of ammonia-oxidizing archaea in water columns and sediments of the ocean, Proc. Natl. Acad. Sci., 102, 14683–14688, https://doi.org/10.1073/pnas.0506625102, 2005.

Fuller, N. J., West, N. J., Marie, D., Yallop, M., Rivlin, T., Post, A. F., Interuniversity, T., Sciences, M., Beach, C., and Scanlan, D. J.: Dynamics of community structure and phosphate status of picocyanobacterial populations in the Gulf of Aqaba , Red Sea, 50, 363–375, 2005.

Grasshoff, K., Kremling, K., and Ehrhardt, M.: Methods of seawater analysis, 3rd ed., edited by: Kremling, K., Ehrenreich, I. M., and Grasshoff, K., Wiley, New York, 632 pp., 1999.

Henriksen, K. and Kemp, W. M.: Nitrification in estuarine and coastal marine sediments, in: Nitrogen Cycling in Coastal Marine Environments, edited by: Blackburn, T. . and Sorensen, J., John Wiley & Sons, Ltd, 207–249, 1988.

Herbert, R. A.: Nitrogen cycling in coastal marine ecosystems, FEMS Microbiol. Rev., 23, 563–590, https://doi.org/10.1111/j.1574-6976.1999.tb00414.x, 1999.

Holms, R. ., Aminot, A., Kérouel, R., Hooker, B. ., and Peterson, B. .: A simple and precise method for measuring ammonium in marine and freshwater ecosystems, Can. Data Rep. Fish. Aquat. Sci., 56, 1801–1808, https://doi.org/10.1139/cjfas-56-10-1801, 1999.

Jiang, M., Koba, K., Ono, M., and Hayashi, K.: Improved isotopic analysis of low-concentration freshwater nitrite by anion-exchange resin enrichment and azide reduction, Anal. Chem., 98, 2956–2967, https://doi.org/10.1021/acs.analchem.5c05937, 2026.

van Kessel, M. A. H. J., Speth, D. R., Albertsen, M., Nielsen, P. H., Op den Camp, H. J. M., Kartal, B., Jetten, M. S. M., and Lücker, S.: Complete nitrification by a single microorganism, Nature, 528, 555–559, https://doi.org/10.1038/nature16459, 2015.

Mackey, K. R. M., Labiosa, R. G., Calhoun, M., Street, J. H., Post, A. F., and Paytan, A.: Phosphorus availability, phytoplankton community dynamics, and taxon-specific phosphorus status in the Gulf of Aqaba, Red Sea, Limnol. Oceanogr., 52, 873–885, https://doi.org/10.4319/lo.2007.52.2.0873, 2007.

Mackey, K. R. M., Bristow, L., Parks, D. R., Altabet, M. A., Post, A. F., and Paytan, A.: The influence of light on nitrogen cycling and the primary nitrite maximum in a seasonally stratified sea, Prog. Oceanogr., 91, 545–560, https://doi.org/https://doi.org/10.1016/j.pocean.2011.09.001, 2011.

Martocello, D. E. and Wankel, S. D.: Physiological influence of Fe and Cu availability on nitrogen isotope fractionation during ammonia oxidation, Environ. Sci. Technol., 58, 421–431, https://doi.org/10.1021/acs.est.3c05964, 2024.

McIlvin, M. R. and Altabet, M. A.: Chemical conversion of nitrate and nitrite to nitrous oxide for nitrogen and oxygen isotopic analysis in freshwater and seawater, Anal. Chem., 77, 5589–

5595, https://doi.org/10.1021/ac050528s, 2005.

Mdutyana, M., Thomalla, S. J., Philibert, R., Ward, B. B., and Fawcett, S. E.: The seasonal cycle of nitrogen uptake and nitrification in the Atlantic sector of the Southern Ocean, Global Biogeochem. Cycles, 34, e2019GB006363, https://doi.org/https://doi.org/10.1029/2019GB006363, 2020.

Meeder, E., MacKey, K. R. M., Paytan, A., Shaked, Y., Iluz, D., Stambler, N., Rivlin, T., Post, A. F., and Lazar, B.: Nitrite dynamics in the open ocean-clues from seasonal and diurnal variations, Mar. Ecol. Prog. Ser., 453, 11–26, https://doi.org/10.3354/meps09525, 2012.

Merbt, S. N., Stahl, D. A., Casamayor, E. O., Martí, E., Nicol, G. W., and Prosser, J. I.: Differential photoinhibition of bacterial and archaeal ammonia oxidation, FEMS Microbiol. Lett., 327, 41–46, https://doi.org/10.1111/j.1574-6968.2011.02457.x, 2012.

Michael Beman, J., Popp, B. N., and Alford, S. E.: Quantification of ammonia oxidation rates and ammonia-oxidizing archaea and bacteria at high resolution in the Gulf of California and eastern tropical North Pacific Ocean, Limnol. Oceanogr., 57, 711–726, https://doi.org/https://doi.org/10.4319/lo.2012.57.3.0711, 2012.

Middelburg, J. J.: Chemoautotrophy in the ocean, Geophys. Res. Lett., 38, 94–97, https://doi.org/10.1029/2011GL049725, 2011.

Mincer, T. J., Church, M. J., Taylor, L. T., Preston, C., Karl, D. M., and DeLong, E. F.: Quantitative distribution of presumptive archaeal and bacterial nitrifiers in Monterey Bay and the North Pacific Subtropical Gyre, Environ. Microbiol., 9, 1162–1175, https://doi.org/https://doi.org/10.1111/j.1462-2920.2007.01239.x, 2007.

Olsen, R.: Differential photoinhibition of marine nitrifying bacteria: a possible mechanism for the formation of the primary nitrite maximum, J. Mar. Syst., 31, 227–238, 1989.

Pachiadaki, M. G., Sintes, E., Bergauer, K., Brown, J. M., Record, N. R., Swan, B. K., Mathyer, M. E., Hallam, S. J., Lopez-Garcia, P., Takaki, Y., Nunoura, T., Woyke, T., Herndl, G. J., and Stepanauskas, R.: Major role of nitrite-oxidizing bacteria in dark ocean carbon fixation, Science (80-.)., 358, 1046–1051, https://doi.org/10.1126/science.aan8260, 2017.

Rahav, E., Herut, B., Mulholland, M. R., Belkin, N., Elifantz, H., and Berman-Frank, I.: Heterotrophic and autotrophic contribution to dinitrogen fixation in the Gulf of Aqaba, Mar. Ecol. Prog. Ser., 522, 67–77, https://doi.org/10.3354/meps11143, 2015.

Reich, T., Belkin, N., Sisma-Ventura, G., Berman-Frank, I., and Rahav, E.: Significant dark inorganic carbon fixation in the euphotic zone of an oligotrophic sea, Limnol. Oceanogr., 9999, 1–14, https://doi.org/10.1002/lno.12560, 2024.

Reich, T., Belkin, N., Sisma-Ventura, G., Hauzer, H., Rubin-Blum, M., Berman-Frank, I., and Rahav, E.: Contribution of dark inorganic carbon fixation to bacterial carbon demand in the oligotrophic Southeastern Mediterranean Sea, Ocean Sci., 21, 3055–3067, https://doi.org/10.5194/os-21-3055-2025, 2025.

Reich, T., Belkin, N., Sisma-ventura, G., Hauzer, H., Berman-frank, I., and Rahav, E.: Does oligotrophy favor chemoautotrophy over photoautotrophy ?, Prog. Oceanogr., 241, 103633, https://doi.org/10.1016/j.pocean.2025.103633, 2026.

Santoro, A. E., Casciotti, K. L., and Francis, C. A.: Activity, abundance and diversity of nitrifying archaea and bacteria in the central California current, Environ. Microbiol., 12,

1989–2006, https://doi.org/https://doi.org/10.1111/j.1462-2920.2010.02205.x, 2010.

Scofield, A. E., Watkins, J. M., Osantowski, E., and Rudstam, L. G.: Deep chlorophyll maxima across a trophic state gradient: A case study in the Laurentian Great Lakes., Limnol. Oceanogr., 65, 2460–2484, https://doi.org/10.1002/lno.11464, 2020.

Shafiee, R. T., Snow, J. T., Zhang, Q., and Rickaby, R. E. M.: Iron requirements and uptake strategies of the globally abundant marine ammonia-oxidising archaeon, Nitrosopumilus maritimus SCM1, ISME J., 13, 2295–2305, https://doi.org/10.1038/s41396-019-0434-8, 2019.

Shafiee, R. T., Diver, P. J., Snow, J. T., Zhang, Q., and Rickaby, R. E. M.: Marine ammonia-oxidising archaea and bacteria occupy distinct iron and copper niches, ISME Commun., 1, 1, https://doi.org/10.1038/s43705-021-00001-7, 2021.

Shiozaki, T., Ijichi, M., Fujiwara, A., Makabe, A., Nishino, S., Yoshikawa, C., and Harada, N.: Factors regulating nitrification in the Arctic Ocean: potential impact of sea ice reduction and ocean acidification, Global Biogeochem. Cycles, 33, 1085–1099, https://doi.org/https://doi.org/10.1029/2018GB006068, 2019.

Sigman, D. M., Casciotti, K. L., Andreani, M., Barford, C., Galanter, M., and Böhlke, J. K.: A bacterial method for the nitrogen isotopic analysis of nitrate in seawater and freshwater, Anal. Chem., 73, 4145–4153, https://doi.org/10.1021/ac010088e, 2001.

Smith, J. M., Damashek, J., Chavez, F. P., and Francis, C. A.: Factors influencing nitrification rates and the abundance and transcriptional activity of ammonia-oxidizing microorganisms in the dark northeast Pacific Ocean, Limnol. Oceanogr., 61, 596–609, https://doi.org/https://doi.org/10.1002/lno.10235, 2016.

Stambler, N.: Light and picophytoplankton in the Gulf of Eilat (Aqaba), J. Geophys. Res., 111, C11009, 2006.

Stambler, N.: Underwater light field of the Mediterranean Sea, in: Life in the Mediterranean Sea: A Look at Habitat Changes, edited by: Stambler, N., Nova Science Publishers, 1–739, 2012.

Steemann-Nielsen, E.: The use of radioactive carbon (14C) for measuring organic production in the sea, J. des Cons. Int. Pour Explor. la Mer, 18, 117–140, 1952.

Stukel, M. R.: Investigating equations for measuring dissolved inorganic nutrient uptake in oligotrophic conditions, Limnol. Oceanogr. Methods, 18, 656–672, 2020.

Suggett, D. J., Stambler, N., Prášil, O., Kolber, Z., Quigg, A., VÃ□Â¡zquez-Dominguez, E., Zohary, T., Berman, T., Iluz, D., Levitan, O., Lawson, T., Meeder, E., Lazar, B., Bar-Zeev, E., Medova, H., and Berman-Frank, I.: Nitrogen and phosphorus limitation of oceanic microbial growth during spring in the Gulf of Aqaba, Aquat. Microb. Ecol., 56, 227–239, 2009.

Tang, W., Ward, B. B., Beman, M., Bristow, L., Clark, D., Fawcett, S., Frey, C., Fripiat, F., Herndl, G. J., Mdutyana, M., Paulot, F., Peng, X., Santoro, A. E., Shiozaki, T., Sintes, E., Stock, C., Sun, X., Wan, X. S., Xu, M. N., and Zhang, Y.: Database of nitrification and nitrifiers in the global ocean, Earth Sci. Rev., 15, 5039–5077, https://doi.org/https://doi.org/10.5194/essd-15-5039-2023, 2023.

Torfstein, A., Teutsch, N., Tirosh, O., Shaked, Y., Rivlin, T., Zipori, A., Stein, M., Lazar, B., and Erel, Y.: Chemical characterization of atmospheric dust from a weekly time series in the

781 north Red Sea between 2006 and 2010, Geochim. Cosmochim. Acta, 211, 373–393,
782 https://doi.org/10.1016/j.gca.2017.06.007, 2017.

783 Travis, N. M., Kelly, C. L., and Casciotti, K. L.: Testing the influence of light on nitrite
784 cycling in the eastern tropical North Pacific, Biogeosciences, 21, 1985–2004,
785 https://doi.org/10.5194/bg-21-1985-2024, 2024.

786 Wan, X. S., Sheng, H.-X., Dai, M., Church, M. J., Zou, W., Li, X., Hutchins, D. A., Ward, B.
787 B., and Kao, S.-J.: Phytoplankton-nitrifier interactions control the geographic distribution of
788 nitrite in the upper ocean, Global Biogeochem. Cycles, 35, e2021GB007072,
789 https://doi.org/https://doi.org/10.1029/2021GB007072, 2021.

790 Wan, X. S., Sheng, H.-X., Shen, H., Zou, W., Tang, J.-M., Qin, W., Dai, M., Kao, S.-J., and
791 Ward, B. B.: Significance of Urea in Sustaining Nitrite Production by Ammonia Oxidizers in
792 the Oligotrophic Ocean, Global Biogeochem. Cycles, 38, e2023GB007996,
793 https://doi.org/https://doi.org/10.1029/2023GB007996, 2024.

794 Wankel, S. D., Kendall, C., Pennington, J. T., Chavez, F. P., and Paytan, A.: Nitrification in
795 the euphotic zone as evidenced by nitrate dual isotopic composition: Observations from
796 Monterey Bay , California, Glob. Biochem. cycles, 21, 1–13,
797 https://doi.org/10.1029/2006GB002723, 2007.

798 Ward, B. B.: Light and substrate concentration relationships with marine ammonium
799 assimilation and oxidation rates, Mar. Chem., 16, 301–316,
800 https://doi.org/https://doi.org/10.1016/0304-4203(85)90052-0, 1985.

801 Ward, B. B.: Nitrogen transformations in the Southern California Bight, Deep Sea Res. Part
802 A. Oceanogr. Res. Pap., 34, 785–805, https://doi.org/https://doi.org/10.1016/0198-
803 0149(87)90037-9, 1987.

804 Ward, B. B.: Nitrification in Marine Systems, in: Nitrogen in the Marine Environment
805 Environment, edited by: Capon, D. G., Bronk, D. A., Mulholland, M. R., and Carpenterl, E.
806 J., Elsevier, 199–262, https://doi.org/10.1016/B978-0-12-372522-6.00005-0, 2008.

807 Welschmeyer, N. A.: Fluorometric analysis of chlorophyll a in the presence of chlorophyll b
808 and pheopigments, Limnol. Oceanogr., 39, 1985–1992, 1994.

809 Wuchter, C., Abbas, B., Coolen, M. J. L., Herfort, L., van Bleijswijk, J., Timmers, P., Strous,
810 M., Teira, E., Herndl, G. J., Middelburg, J. J., Schouten, S., and Sinninghe Damsté, J. S.:
811 Archaeal nitrification in the ocean, Proc. Natl. Acad. Sci., 103, 12317–12322,
812 https://doi.org/10.1073/pnas.0600756103, 2006.

813 Xu, M. N., Li, X., Shi, D., Zhang, Y., Dai, M., Huang, T., Glibert, P. M., and Kao, S.-J.:
814 Coupled effect of substrate and light on assimilation and oxidation of regenerated nitrogen in
815 the euphotic ocean, Limnol. Oceanogr., 64, 1270–1283,
816 https://doi.org/https://doi.org/10.1002/lno.11114, 2019.

817 Yin, Q., He, K., Collins, G., De Vrieze, J., and Wu, G.: Microbial strategies driving low
818 concentration substrate degradation for sustainable remediation solutions, npj Clean Water, 7,
819 52, https://doi.org/10.1038/s41545-024-00348-z, 2024.

820 Yool, A., Martin, A. P., Fernández, C., and Clark, D. R.: The significance of nitrification for
821 oceanic new production, Nature, 447, 999–1002, https://doi.org/10.1038/nature05885, 2007.

822 Zheng, Z.-Z., Wan, X., Xu, M. N., Hsiao, S. S.-Y., Zhang, Y., Zheng, L.-W., Wu, Y., Zou,
823 W., and Kao, S.-J.: Effects of temperature and particles on nitrification in a eutrophic coastal

bay in southern China, J. Geophys. Res. Biogeosciences, 122, 2325–2337, https://doi.org/https://doi.org/10.1002/2017JG003871, 2017.

Zheng, Z.-Z., Zheng, L.-W., Xu, M. N., Tan, E., Hutchins, D. A., Deng, W., Zhang, Y., Shi, D., Dai, M., and Kao, S.-J.: Substrate regulation leads to differential responses of microbial ammonia-oxidizing communities to ocean warming, Nat. Commun., 11, 3511, https://doi.org/10.1038/s41467-020-17366-3, 2020.

Zhou, Y., Yan, A., Yang, J., He, W., Guo, S., Li, Y., Wu, J., Dai, Y., Pan, X., Cui, D., Pereira, O., Teng, W., Bi, R., Chen, S., Fan, L., Wang, P., Liao, Y., Qin, W., Sui, S.-F., Zhu, Y., Zhang, C., and Liu, Z.: Ultrastructural insights into cellular organization, energy storage and ribosomal dynamics of an ammonia-oxidizing archaeon from oligotrophic oceans, Front. Microbiol., 15, 1367658, https://doi.org/10.3389/fmicb.2024.1367658, 2024.

Zhu, W., Wang, C., Hill, J., He, Y., Tao, B., Mao, Z., and Wu, W.: A missing link in the estuarine nitrogen cycle? Coupled nitrification-denitrification mediated by suspended particulate matter, Sci. Rep., 8, 2282, https://doi.org/10.1038/s41598-018-20688-4, 2018.